China Petroleum Processing and Petrochemical Technology

Catalyst Research Volume 23, Issue 2, November 2023 Pp. 3800-3811

SYNTHESIS, CHARACTERIZATION AND DFT STUDIES OF 4-FLUORO-1-(4-FLUOROBENZYL)-2-(4-FLUOROPHENYL)-1*H*-BENZO[D]IMIDAZOLE AS POTENTIAL NLO MATERIAL

K. Kadambary

Department of Chemistry, C. Kandaswami Naidu College for Women, Cuddalore 607001, Tamil Nadu, India.

P.R. Rajakumar

Periyar Arts College, Cuddalore. 607001, Tamil Nadu, India.

M. Sekar*

*PG & Research Department of Chemistry, Government arts College, C. Mutlur 608102, Tamil Nadu, India.

***Corresponding Author:** M. Sekar

* Associate Professor & Head, PG & Research Department of Chemistry, Government arts College, C. Mutlur 608102, Tamil Nadu, India. Mail id: *drmspartha@gmail.com*

Abstract

4-fluoro-1-(4-fluorobenzyl)-2-(4-fluorophenyl)-1*H*-benzo[d]imidazole (FFFB) was designed, prepared and analyzed by spectral studies and CHN elemental analysis. Electric dipole moment (μ) and hyperpolarisability (β) were determined which shows that the synthesized FFFB possess NLO property. This benzimidazole moiety having appropriate ratio of off-diagonal versus diagonal β tensorial component ($r = \beta_{xyy} / \beta_{xxx} = -0.4799$) which reflects the in plane non-linearity anisotropy. Because they have biggest $\mu\beta_0$, the organized FFFB can be used as NLO fabric. within this context, reasonable conclusions regarding the steric challenge within the chromospheres, push-pull character, hyperpolarisability of the imidazole and their application as NLO substances can be drawn.The energy difference between the HOMO and LUMO levels significantly influences the electron-donating and accepting properties, as well as the optical properties. In NBO analysis, significant interaction energies were observed for the same kind of transitions involving electron-donor to electron-acceptor interactions.

Keywords: *NLO material*; *electron-acceptor interactions*; *HOMO- LUMO*; *Benzimidazole*.

1. Introduction

Numerous natural products and pharmaceutically active molecules have the imidazole ring as a significant moiety. There has always been a special place in the world of medicinal chemistry for imidazole derivatives. Fungicidal, antibacterial, anticancer, antiinflammatory, antioxidative, fungicide, herbicide, and therapeutic actions are only some of the various biological activities

shown by imidazole derivatives [1-3]. Excellent linear and non-linear characteristics have attracted more and more research interest in chromophores based on imidazoles. The synthesis of imidazoles is now a major research focus due to their diverse pharmacological, biological and optical characteristics.The linear and non-linear characteristics of chromophores based on the imidazole group have attracted a lot of interest recently [4]. These days, it's all about synthesising imidazoles for their many useful pharmacological, biological, and optical characteristics.

Although organic materials are so versatile, they are the primary raw material for NLO. Delocalization and intermolecular charge transfer inside the molecule trigger a strong NLO reaction, with the impact being exacerbated by hydrogen bonding. Unlike their inorganic cousins, NLOs made from organic materials have a significant nonlinearity and electro-optic influence [5]. Finding a superior organic NLO material to fulfil the needs of modern technology is, therefore, desirable. Researchers are interested in Imidazole and its derivatives because of its unique chemical, biological, pharmacological, and physicochemical features. Density functional theory (DFT) simulations were used to get insight into the reactive properties of newly synthesised imidazole-based derivatives. The reactive qualities of the synthesised derivatives have been calculated, allowing for ecologically appropriate assessments of their degrading qualities. Hence, efforts have been taken to synthesise the benzimidazole and their derivatives using various synthetic routes [6-9]. Anyhow the conventional synthetic routes may encounter practical difficulties such as longer reaction time, formation of by products or mixture of products, reduction in the expected yield, maintaining the vigorous reaction parameters, usage of toxic catalysts and hazardous solvents [10]. To overcome such drawbacks, using heterogeneous metal oxide catalysts are suggested as better alternatives [11].

2. Experimental

2.1. Computational details

Quantum mechanical calculations were used to carry out the optimized geometry, NLO, NBO and HOMO-LUMO analysis with Guassian-03 program using the Becke3-Lee-Yang-Parr (B3LYP) functional supplemented with the standard 6-31G (d, p) basis set [12]. As the first step of our DFT calculation for NLO, NBO and HOMO-LUMO analysis, the geometry taken from the starting structures were optimized and then, the electric dipole moment μ and β tensor components of the studied compounds were calculated, which has been found to be more than adequate for obtaining reliable trends in the first hyperpolarizability values.

We have reported the β_{tot} (total first hyperpolarizability) for the investigated molecules and the components of the first hyperpolarizability can be calculated using equation:

$$\beta_i = \beta_{iii} + 1/3 \sum_{i \neq j} (\beta_{ijj} + \beta_{jij} + \beta_{jji}) \quad (1)$$

Using the *x*, *y* and *z* components, the magnitude of the first hyperpolarizability tensor can be calculated by

$$\beta_{tot} = \left(\beta_x^2 + \beta_y^2 + \beta_z^2\right)^{1/2} \quad (2)$$

The complete equation for calculating the magnitude of first hyperpolarizability from Gaussian-03 output is given as follows:

$$\beta_{tot} = [(\beta_{xxx} + \beta_{xyy} + \beta_{xzz})^2 + (\beta_{yyy} + \beta_{yzz} + \beta_{yxx})^2 + (\beta_{zzz} + \beta_{zxx} + \beta_{zyy})^2]^{1/2} \quad (3)$$

All the electric dipole moment and the first hyperpolarizabilities are calculated by taking the Cartesian coordinate system (x, y, z) = (0, 0, 0) at own center of mass of the compounds.

2.2.1. Natural Bond Orbital (NBO) analysis

NBO analysis have been performed on the molecule at the DFT/B3LYP/6-31G(d,p) level in order to elucidate the intramolecular, rehybridization and delocalization of electron density within the molecule. The second order Fock matrix was carried out to evaluate the donor–acceptor interactions in the NBO analysis. The interactions result is a loss of occupancy from the localized NBO of the idealized Lewis structure into an empty non-Lewis orbital. For each donor (i) and acceptor (j), the stabilization energy E(2) associated with the delocalization i → j is estimated as

$$E^{(2)} = \Delta E_{ij} = q_i \frac{F(i,j)^2}{\varepsilon j - \varepsilon i} \quad (4)$$

Where q_i is the donor orbital occupancy, εi and εj are diagonal elements and F (i, j) is the off diagonal NBO Fock matrix element. The larger the E(2)value, the more intensive is the interaction between electron donors and electron acceptors, i.e., the more donating tendency from electron donors to electron acceptors and the greater the extent of charge transfer or conjugation of the whole system.

2.2 *Synthesis of 4-fluoro-1-(4-fluorobenzyl)-2-(4-fluorophenyl)-1H-benzo[d]imidazole*

4-fluoro-1-(4-fluorobenzyl)-2-(4-fluorophenyl)-1H-benzo[d]imidazole(FFFB)was synthesized by three component assembling of 3-fluorobenzene-1,2-diamine, 4-fluoro benzaldehyde and ammonium acetate in the ratio of 1:2:1 in presence of in the presence of ZnO nano catalyst at 353 K. Yield: 98%. mp. 214 °C, Anal. calcd. for $C_{20}H_{13}F_3N_2$: C: 71.00, H: 3.87, N: 8.28, F: 16.85. Found: C: 71.10, H: 3.77, N: 8.29, F: 16.84. ^{1}H NMR (500 MHz, $CDCl_3$): δ 5.79 (s, 2H) methylene protons, 6.97 - 7.51 (m, 9 H), 8.28 (q, 2 H). ^{13}C (100 MHz, $CDCl_3$): δ 52.2 (methylene carbon), 105.7, 108.9, 123.6, 124.9, 125.9, 126.9, 127.6, 131.1, 128.6, 129.2, 130.6, 135.8, 148.3, 156.0, 157.3.

3. Results and Discussion

3.1 Mulliken Charge Distribution

The electrical charge of an atom determines its ability to create bonds and influences the structure of a molecule[13-15]. Using Mulliken population analysis, the atomic charge values were

Catalyst Research Volume 23, Issue 2, November 2023 Pp. 3800-3811

computed. The calculated atomic charges of the title compound are presented in **Table 1** and graphically represented **in Fig. 1**.

Table 1: Mulliken atomic charges of FFFB

Atoms with numbering	Mulliken atomic charges	Atoms with numbering	Mulliken atomic charges
1 C	0.021403	14 C	-0.02546
2 C	0.07793	15 C	0.1578
3 C	0.064655	16 C	-0.06632
4 C	0.167479	17 C	-0.03372
5 C	0.007824	18 C	0.036417
6 C	-0.05644	19 C	-0.00481
7 N	-0.2636	20 C	0.121765
8 C	0.231561	21 C	-0.04438
9 N	-0.21935	22 C	-0.01691
10 C	0.015492	23 F	-0.08724
11 C	0.122499	24 F	-0.06597
12 C	-0.08247	25 F	-0.08245
13 C	0.024304	-	-

During the current research, it has been seen that some carbon atoms have positive potential when they are joined to fluorine or nitrogen atoms. In particular, the carbon atoms at positions 4C, 15C, and 20C, as well as positions 2C, 3C, 8C, and 11C, have a higher positive potential than other carbon atoms in the compound. The most positive potential is shown by the carbon atom at position 8C, which is between two nitrogen atoms (7N and 9N). This increased positive potential is due to the effect of the nitrogen atoms next to it.On the other hand, it makes sense that the nitrogen atoms at positions 7N and 9N and the fluorine atoms at positions 23F, 24F, and 25F have a more negative potential. Also, compared to the other carbon atoms in the compound, the carbon atom at position 12C has a more negative potential. **Figure 1** shows these differences in potential in a clear way, showing the charges of the atoms involved.

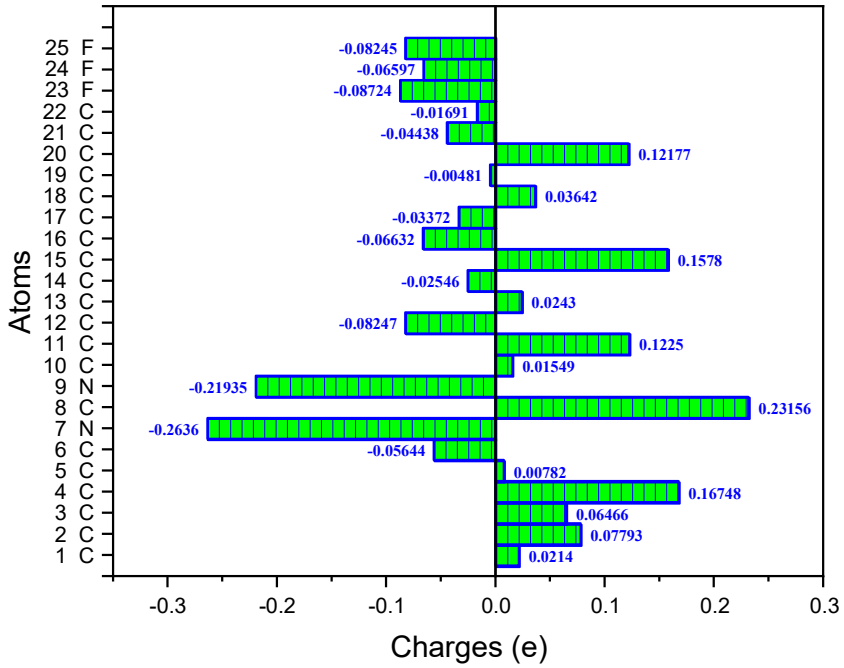

Fig. 1. Calculated atomic charges of FFFB

3.2 HOMO – LUMO

The energies of the highest occupied molecular orbital (HOMO) and the lowest unoccupied molecular orbital (LUMO) play a fascinating role in determining molecules' physical and chemical characteristics. The energy difference between the HOMO and LUMO levels significantly influences the electron-donating and accepting properties, as well as the optical properties [16-18]. In the HOMO-LUMO map, the red and green colours represent the positive and negative regions, respectively, in the compound mentioned. **Table 2** and **Fig. 2** display the energy gaps observed in the gas phase. The electronic properties of the compound primarily involve the transition from the ground state to the first excited state, which is explained by the excitation of a single electron within the energy range of 2.693 eV to -4.816 eV, as well as the molecule's interaction with other groups. The energy gap is determined to be 7.509 eV, confirming the occurrence of charge transfer within the molecule.

Table 2 HOMO – LUMO parameters of FFFB	
Parameters	(eV)
HOMO energy	- 4.816
LUMO energy	2.693
HOMO-LUMO energy gap	7.509
HOMO-1 energy	- 4.979

LUMO+1 energy	3.129
(HOMO-1)-(LUMO+1) energy gap	8.108

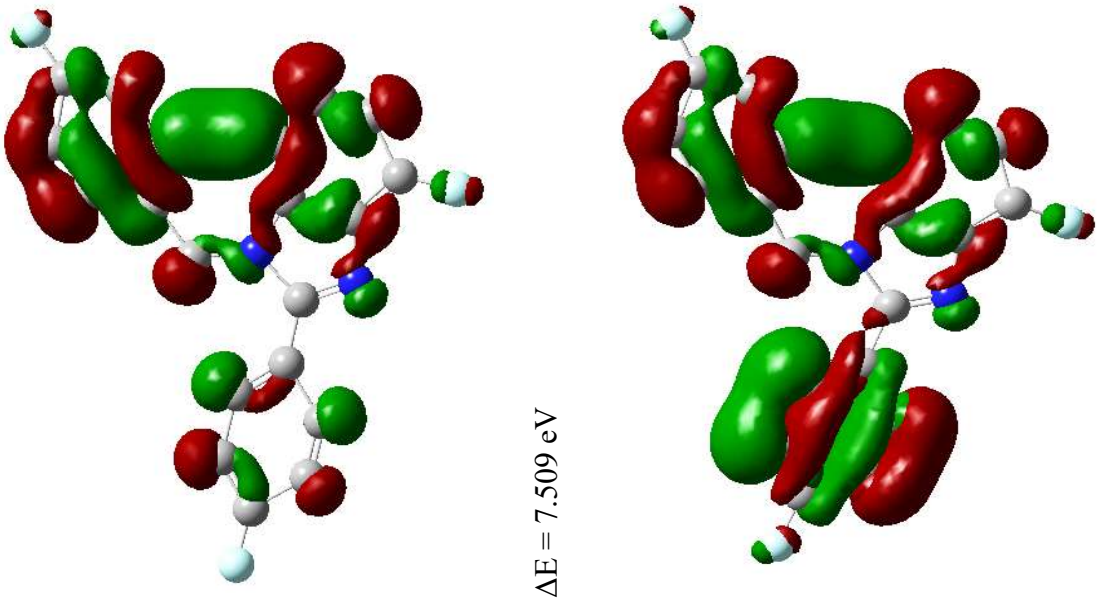

E_{HOMO} = - 4.816 eV E_{LUMO} = 2.693 eV

Fig. 2. The HOMO-LUMO plots of FFFB

3.3. Nonlinear Optical Properties (NLO)

When electromagnetic fields interact with materials, NLO effects result in the generation of new fields with distinct properties. These effects have significant applications in numerous technologies, including optical and telecommunications devices. Presently, NLO research is at the forefront of scientific inquiry. Quantum chemical computations aid in comprehending the relationship between the electronic structure of a system and its NLO response. By analysing their potential and determining their high-order hyperpolarizability tensors, this computational method offers a cost-effective way to design molecules [19-21]. In the present case, the NLO properties of electric dipole moment (μ), polarizability (α) and hyperpolarizability (β) of the title compound are presented in **Table 3**.

Table 3 Electric dipole moment (μ), Polarizability (α) and Hyperpolarizability (β) of FFFB

Parameters	B3LYP/***
Electric dipole moment (μ)	
μ_x	-1.5491
μ_y	-0.9194
μ_z	0.0000
μ_{total}	1.8014

Polarizability (α)	
α_{xx}	-123.5214
α_{xy}	6.8059
α_{yy}	-133.1488
α_{xz}	0.0000
α_{yz}	0.0000
α_{zz}	-120.8174
α_{total} x 10^{-21} (esu)	186.479
Hyperpolarizability (β)	
β_{xxx}	-48.8371
β_{xxy}	-4.6926
β_{xyy}	23.4364
β_{yyy}	-9.3681
β_{xxz}	0.0000
β_{xyz}	0.0000
β_{yyz}	0.0000
β_{xzz}	0.3745
β_{yzz}	0.7406
β_{zzz}	0.0000
β_{total} x 10^{-32} (esu)	24.7787

The total dipole moment was found to be 1.8014 D, and the total polarizability was found to be 186.479 x 10^{-21} e.s.u., which is greater than urea. The value of hyperpolarizability was found to be 24.7787 x 10^{-32} e.s.u. which is greater than the value of urea. Due to its properties, it is a highly promising option for future investigations in the field of non-linear optics.

3.4. Natural Bond Orbital

Natural Bond Orbital (NBO) analysis enables the investigation of donor-acceptor energy interactions, the determination of bond order, natural atomic orbital occupancies, and the application of second-order perturbation theory [22-24]. Using the DFT/B3LYP/ 6-311G++(d,p) level of theory, the NBO analysis was performed on the subject compound in the gas phase the purposes of this study. The investigation's findings are presented in **Table 4.** The transition of π - π* from C14-C16 to C15-C16 contributes the highest stabilizing energy, which has been identified at 25.90 kJ mol^{-1}. Additionally, significant interaction energies were observed for the same kind of transitions involving electron-donor to electron-acceptor interactions, such as C10-C17 to C13-C17, C13-C17 to C10-C17, C15-C16 to C14-C16,C14-C16 to C14-C15, C14-C16 to C15-F24, and C13-C17 to C10-C13 with stabilizing energies of 24.97, 24.23, 24.16, 15.26, 15.12, and 14.47 kJ mol^{-1}, respectively, in the title compound. These findings provide important insights into the rehybridization, delocalization, and intramolecular interactions occurring within the molecule.

Table 4 Natural Bond Orbital (NBO) analysis of FFFB

Donor(i)	Type	ED/e	Acceptor(J)	Type	ED/e	$E^{(2)}$ kcal/mol	$E_{(j)}$-$E_{(i)}$ a.u.	$F_{(i, j)}$ a.u.
C1 - C2	π	0.988	C1 - C18	π*	0.1371	2.47	1	0.07
C1 - C18	π	0.9459	C1 - C6	π*	0.0236	5.08	1	0.09
	π	0.9459	C2 - C3	π*	0.0271	5.06	0.85	0.08
	π	0.9459	C2 - N7	π*	0.0237	3.67	0.9	0.07
	π	0.9459	C12 - C18	π*	0.0656	6.52	1.14	0.11
C2 - C3	π	0.9738	C1 - C18	π*	0.1371	5.37	0.78	0.09
C3 - C4	π	0.9823	C4 - F23	π*	0.015	2.93	1.4	0.08
	π	0.9823	C5 - C6	π*	0.0129	3.03	1.26	0.08
C4 - C5	π	0.9854	C5 - C6	π*	0.0129	3.01	1.66	0.09
N7 - C11	π	0.9846	N7 - C8	π*	0.0333	3.61	1.37	0.09
C10 - C17	π	0.9378	C13 - C17	π*	0.1045	24.97	0.84	0.19
C11 - C12	π	0.9842	N7 - C11	π*	0.0135	3.54	1.33	0.09
C12 - C22	π	0.9551	C1 - C18	π*	0.1371	6.98	0.76	0.1
C13 - C14	π	0.9588	C10 - C13	π*	0.0751	4.81	1.6	0.11
	π	0.9588	C13 - C17	π*	0.1045	7.4	0.89	0.11
	π	0.9588	C14 - C15	π*	0.0435	4.61	1.57	0.11
	π	0.9588	C14 - C16	π*	0.0435	7.28	0.89	0.11
C13 - C17	π	0.8992	C8 - C10	π*	0.0245	10.64	0.78	0.12
	π	0.8992	C10 - C13	π*	0.0751	14.47	1.01	0.16
	π	0.8992	C10 - C17	π*	0.0532	24.23	0.77	0.18
C14 - C16	π	0.8971	C14 - C15	π*	0.0435	15.26	0.99	0.16
	π	0.8971	C15 - C16	π*	0.0667	25.9	0.75	0.18
	π	0.8971	C15 - F24	π*	0.0205	15.12	0.74	0.14
C15 - C16	π	0.9393	C14 - C16	π*	0.1046	24.16	0.86	0.19

Catalyst Research Volume 23, Issue 2, November 2023 Pp. 3800-3811

3.5 Comparison of μβ₀

The overall polarity of the synthesized imidazole spinoff turned into small when their dipole moment aligned in a parallel style.whilst the electric field is eliminated, the parallel alignment of the molecular dipole moments starts to become worse and in the end the imidazole spinoff loses its NLO interest. The last aim within the layout of polar materials is to prepare compounds that have their molecular dipole moments aligned within the equal route.

Theoretical investigation plays an important role in understanding the structure-property relationship, which is able to assist in designing novel NLO chormophores. The electrostatic first hyperpolarizability (β) and dipole moment (μ) of the imidazole chromophore have been calculated by using Gaussian 03 package [12]. From Table 3, it is found that the imidazole chromophore show larger $\mu_g\beta_o$ values, which is attributed to the positive contribution of their conjugation. This chromophore exhibits larger non-linearity and its λ_{max} is red-shifted when compared with unsubstituted imidazole. Therefore, it is clear that the hyperpolarizability is a strong function of the absorption maximum. Since even a small absorption at the operating wavelength of optic devices can be detrimental, it is important to make NLO chromophores as transparent as possible without compromising the molecule's non-linearity.

3.6 Octupolar and dipolar components of FFFB

FFFB possess a more appropriate ratio of off-diagonal versus diagonal β tensorial component (r =$\beta_{xyy}/\beta xxx$) which reflects the inplane non-linearity anisotropy and the largest $\mu\beta_o$ values. The difference of the β_{xyy}/β_{xxx} ratios can be well understood by analyzing their relative molecular orbital properties. The electrostatic first hyperpolarizabilities (β_0) and dipole moment (μ) of the chromophores have been investigated theoretically. These observed results can be explained by the reduced planarity in such chromophores caused by the steric interaction between the two phenyl rings at carbon and nitrogen. Hence, the steric interaction must be reduced in order to obtain larger β_0 values.

The β tensor can be decomposed in a sum of dipolar ($\|_{J=1}^{2D}\beta\|$) and octupolar ($\|_{J=3}^{2D}\beta\|$) tensorial components, and the ratio of these two components strongly depends on their 'r' ratios. The zone for $r > r_2$ and $r < r_1$ corresponds to a molecule of octupolar and dipolar respectively. The critical values for r_1 and r_2 are $(1-\sqrt{3})/\sqrt{3}\sqrt{3}+1) = -0.16$ and $(\sqrt{3}+1)/\sqrt{3}(\sqrt{3}-1) = 2.15$, respectively. Complying with the Pythagorean theory and the projection closure condition, the octupolar and dipolar components of the β tensor can be described as:

$$\|_{J=1}^{2D}\beta\| = (3/4)[(\beta_{xxx} + \beta_{xyy})^2 + [(\beta_{yyy} + \beta_{yxx})^2 \ ] \quad (6)$$

$$\|_{J=3}^{2D}\beta\| = (1/4)[(\beta_{xxx} - 3\beta_{xyy})^2 + [(\beta_{yyy} - \beta_{yxx})^2 \ ] \quad (7)$$

The parameter ρ^{2D} [$\rho^{2D} = \frac{\|_{J=3}^{2D}\beta\|}{\|_{J=1}^{2D}\beta\|}$] is convenient to compare the relative magnitudes of the octupolar and dipolar components of β. The observed positive small ρ^{2D} value reveals that the β_{iii}

component cannot be zero and these are dipolar component. Since most of the practical applications for second order NLO chromophores are based on their dipolar components, this strategy is more appropriate for designing highly efficient NLO chromophores.

4. Conclusions

4-fluoro-1-(4-fluorobenzyl)-2-(4-fluorophenyl)-1H-benzo[d]imidazole (FFFB) has been synthesized by easy and an green route and it's been charactreized by way of proton NMR, carbon NMR, mass spectral stuides and elemetal analysisTheoretical investigation plays an critical position in knowledge the shape-assets courting, that's capable of assist in designing novel NLO chormophores. The found dipole moment and hyperpolarisability can be explained with the aid of the decreased planarity as a result of the steric interaction among the 2 phenyl rings. The total dipole moment changed into discovered to be 1.8014 D, and the total polarizability became found to be -186.47 x 10-21e.s.u. additionally, sizeable interaction energies had been observed for the identical sort of transitions involving electron-donor to electron-acceptor interactions, which include C10-C17 to C13-C17, C13-C17 to C10-C17, C15-C16 to C14-C16,C14-C16 to C14-C15, C14-C16 to C15-F24, and C13-C17 to C10-C13 with stabilizing energies of 24.ninety seven, 24.23, 24.sixteen, 15.26, 15.12, and 14.47 kJ mol-1, respectively, within the identify compound. The electronic residences of imidazole correspond to the transition from ground to the first excited kingdom, which is basically defined through one electron excitation among - 4.816 eV and 2.693 eV as well as the manner of molecule interplay with different groups.

References

1. Jayabharathi J, Thanikachalam V, Jayamoorthy K, PhotochemJ (2012) Photobiol B 115:85–92.
2. Mahal K, Biersack B, Schruefer S, Resch M, Ficner R, Schobert R, Mueller T (2016) Eur J Med Chem 118:9–20.
3. Mahal K, Kahlen P, Biersack B, Schobert R (2015) Exp Cell Res336:263–275.
4. Kaps L, Biersack B, Muller-Bunz H, Mahal K, M ¨ unzner J, Tacke M, Mueller T, Schobert R (2012) J Inorg Biochem106:52–58.
5. Biersack B, Muthukumar Y, Schobert R, Sasse F (2011) Bioorg Med Chem Lett 21: 6270–6273.
6. Mohammadpoor-Baltork, A.R. Khosropour, S.F. Hojati, Cata. Commun.8 (2007) 1865 e18 70.
7. Y. Kim, M.R. Kumar, N. Park, Y. Heo, S. Lee, J. Org. Chem. 76 (2011) 9577e9583.
8. K. Bahrami, M.M. Khodaei, I. Kavianinia, J. Chem. Res. 2006 (2006) 783e784.
9. L.H. Du, Y.G. Wang, Synthesis (2007) 675e678
10. Leila Dinparast, Hassan Valizadeh, Mir BabakBahadori, Somaieh Soltani, Behvar Asghari, Mohammad-RezaRashidi, Design, synthesis, a-glucosidase inhibitory activity, molecular

docking and QSAR studies of benzimidazole derivatives, Journal of Molecular Structure 1114 (2016) 84-94
11. K. Sivakumar, V. Senthil Kumar, J.J. Shim, Y. Haldorai, Synth. React. Inorg.Met. Org. Nano-Met. Chem. 45 (2015) 660-666.
12. Frisch, M. J.; Trucks, G. W.; Schlegel, H. B.; Scuseria, G. E.; Robb, M. A.; Cheeseman, J. R.; Montgomery, J. A.; Vreven, T., Jr.; Kudin, K. N.; Burant, J. C.; Millam, J. M.; Iyengar, S. S.; Tomasi, J.; Barone, V.; Mennucci, B.; Cossi, M.; Scalmani, G.; Rega, N.; Petersson, G. A.; Nakatsuji, H.; Hada, M.; Ehara, M.; Toyota, K.; Fukuda, R.; Hasegawa, J.; Ishida, M.; Nakajima, T.; Honda, Y.; Kitao, O.; Nakai, H.; Klene, M.; Li, X.; Knox, J. E.; Hratchian, P.; Cross, J. B.; Adamo, C.; Jaramillo, J.; Gomperts, R.; Stratmann, R. E.; Yazyev, O.; Austin, A. J.; Cammi, R.; Pomelli, C.; Ochterski, J.W.; Ayala, P. Y.; Morokuma, K.; Voth, G. A.; Salvador, P.; Dannenberg, J. J.; Zakrzewski, V. G.; Dapprich, S.; Daniels, A. D.; Strain, M. C.; Farkas, O.; Malick, D. K.; Rabuck, A. D.; Raghavachari, K.; Foresman, J. B.; Ortiz, J. V.; Cui, Q.; Baboul, A. G.; Clifford, S.; Cioslowski, J.; Stefanov, B. B.; Liu, G.; Liashenko, A.; Piskorz, P.; Komaromi, I.; Martin, R. L.; Fox, D. J.; Keith, T.; Al-Laham, M. A.; Peng, C. Y.; Nanayakkara, A.; Challacombe, M.; Gill, P. M. W.; Johnson, B.; Chen, W.; Wong, M. W.; Gonzalez, C.; Pople, J. A. Gaussian 03, Revision C.02, Gaussian, Inc.: Wallingford, CT, 2004.
13. S. Selvaraj, P. Rajkumar, M. Kesavan, K. Mohanraj, S. Gunasekaran, S. Kumaresan, A combined experimental and theoretical study on 4-hydroxy carbazole by FT-IR, FT-Raman, NMR, UV–visible and quantum chemical investigations, Chem. Data. Collect. 17 (2018) 302-311.
14. Ram Kumar, S. Selvaraj, K.S. Jayaprakash, S. Gunasekaran, S. Kumaresan, J. Devanathan, K.A. Selvam, L. Ramadass, M. Mani, P. Rajkumar, Multi-spectroscopic (FT-IR, FT-Raman, 1H NMR and 13C NMR) investigations on syringaldehyde, J. Mol. Struct. 1229 (2021) 129490.
15. S. Selvaraj, A. Ram Kumar, T. Ahilan, M. Kesavan, S. Gunasekaran, S. Kumaresan, Multi spectroscopic and computational investigations on the electronic structure of oxyclozanide, J. Indian Chem. Soc. 99 (2022) 100676.
16. S. Selvaraj, P. Rajkumar, M. Kesavan, K. Thirunavukkarasu, S. Gunasekaran, N.S. Devi, S. Kumaresan, Spectroscopic and structural investigations on modafinil by FT-IR, FT-Raman, NMR, UV–Vis and DFT methods, Spectrochim. Acta A. Mol. Biomol. Spectrosc. 224 (2020) 117449, DOI: https://doi.org/10.1016/j.saa.2019.117449.
17. J. Jayabharathi, V. Thanikachalam, N. Srinivasan, M. Venkatesh Perumal, K. Jayamoorthy, Physicochemical studies of molecular hyperpolarizability of imidazole derivatives, Spectrochimica Acta Part A: Molecular and Biomolecular Spectroscopy, 79, 2011, 137-147.
18. J Jayabharathi, V Thanikachalam, M Vennila, K Jayamoorthy, Potential fluorescent chemosensor based on L-tryptophan derivative: DFT based ESIPT process, Spectrochimica Acta Part A: Molecular and Biomolecular Spectroscopy 95, 2012, 446-451
19. Ram Kumar, N. Kanagathara, S. Selvaraj, Spectroscopic, Structural and Molecular Docking Studies on N, N-Dimethyl-2-[6-methyl-2-(4-methylphenyl) Imidazo [1,2-a] pyridin-3-yl]

Acetamide, Phys. Chem. Res. 12 (2024) 95-107, DOI: https://doi.org/10.22036/PCR.2023.387911.2306
20. S. Selvaraj, P. Rajkumar, M. Kesavan, S. Gunasekaran, S. Kumaresan, R. Rajasekar, T.R. Devi, Spectroscopic and quantum chemical investigations on structural isomers of dihydroxybenzene, J. Mol. Struct. 1196 (2019) 291-305, DOI: https://doi.org/10.1016/j.molstruc.2019.06.075
21. N. Kanagathara, M. Thirunavukkarasu, S. Selvaraj, A. Ram Kumar, M. Marchewka, J. Janczak, Structural elucidation, solvent (polar and non-polar) effect on electronic characterization, non-covalent charge interaction nature, topology and pharmacological studies on NLO active l-argininium methanesufonate, J. Mol. Liq. 385 (2023) 122315, DOI: https://doi.org/10.1016/j.molliq.2023.122315.
22. J Jayabharathi, V Thanikachalam, K Jayamoorthy, Physicochemical studies of chemosensor imidazole derivatives: DFT based ESIPT process, Spectrochimica Acta Part A: Molecular and Biomolecular Spectroscopy 89, 2012, 168-176.
23. J Jayabharathi, V Thanikachalam, V Kalaiarasi, K Jayamoorthy, Optical properties of 1-(4,5-diphenyl-1-p-tolyl-1H-imidazol-2-yl)naphthalen-2-ol–ESIPT process, Spectrochimica Acta Part A: Molecular and Biomolecular Spectroscopy 120, 2014, 389-394.
24. J Jayabharathi, V Thanikachalam, K Jayamoorthy, MV Perumal, A physiochemical study of excited state intramolecular proton transfer process: luminescent chemosensor by spectroscopic investigation supported by ab initio calculations, Spectrochimica Acta Part A: Molecular and Biomolecular Spectroscopy 79 (1), 2011, 6-16.